Climate Surfaces for the Okanagan Basin Water Supply Demand Project

Guy Duke, Denise Neilsen, Bill Taylor, Alex Cannon, Ted Van der Gulik, Nathanial Newlands, Grace Frank, and Scott Smith

Abstract

The diverse terrain of the Okanagan Basin has a strong localizing influence on climate. Model development for water supply and demand requires climate data inputs that reflect this complexity. The Okanagan Climate Data Model has been developed to provide climate information at a suitable scale for modelling climate dependent processes. Using GIS interpolation methodology and all available climate data from a number of sources, basin-wide 500m x 500m gridded surfaces for daily minimum, maximum temperatures and precipitation have been generated for the period 1960 to 2000. Future daily climate data, up to the year 2100, have also been generated using output from six Global Climate Models (GCM) and three SRES scenarios reflecting high and low greenhouse gas emissions. GCM output has been downscaled to climate grid cells using a combined synoptic map typing and weather generator approach.

The Okanagan Climate Data Model has been used to drive the Okanagan Irrigation Water Demand Model, which provides calculations of Penman Monteith reference ET and a range of agro-climatic indices for each climate grid cell in addition to crop and terrain based irrigation water demand.

Introduction

The terrain of the Okanagan Basin is diverse and has a strong influence on climate. Water supply and demand models require climate data inputs that reflect this complexity, but climate stations are few and located mainly in the valley bottom. Consequently, spatial interpolation at a suitable scale is required to fill in gaps in temperature and precipitation data. A number of approaches have been used previously to develop models which incorporate spatial correlation and topographic effects on climate data. These include GIDS (Gradient plus Inverse-Distance-Squared) which weights predictions derived from a multiple regression equation with the inverse distance to nearby climate stations within a specified search radius (Nalder and Wein, 1998) and

Guy Duke[1], Denise Neilsen[2], Bill Taylor[3], Alex Cannon[3], Ted Van der Gulik[4], Nathanial Newlands[5], Grace Frank[2] and Scott Smith[2]

[1] University of Lethbridge, Lethbridge, AB.
[2] Agriculture and Agri-Food Canada, Pacific Agri-Food Research Centre, Summerland BC
Corresponding Author: Denise Neilsen, neilsend@agr.gc.ac, 250-494-6417
[3] Environment Canda, Pacific andYukon Region, Vancouver, BC
[4] BC Ministry of Agriculture and Lands, Abbotsford, BC
[5] Agriculture and Agri-Food Canada, Lethbridge, AB

PRISM (Parameter-elevation Regressions on Independent Slopes Model) Daly *et al.* (1994) with a search neighbourhood limited to climate located on the same topographic facet (i.e., a common aspect). Other approaches include DAYMET (DAilY METeorology) (Thornton *et al.*, 1997) which uses weighted observed climate values within a search radius using a Gaussian filter with a shape parameter and ANUSPLIN (Australian National University SPLINe) Hutchinson (1995, 1999) which uses a thin plate spline algorithm to fit a smooth surface through data values. Each of these methods has shortcomings in mountainous regions where terrain variations have a substantial effect on local climate.

To account for temperature inversions, efforts have also been made to utilize two atmospheric layers when deriving gridded temperature datasets. Using PRISM, Daly *et al.* (2003) divided meteorological point data into two sets and used weighting factors to limit the ability of stations above an inversion to influence the climate parameters within the mixed layer. A standard inversion height (based on radiosonde data) and predefined inversion locations were specified (Daly *et al.*, 2003). The PRISM two layer approach has been successfully applied across North America (Daly *et al.*, 1994, 2003; Simpson *et al.*, 2005).

In addition to terrain, large water bodies can also influence climate patterns significantly. Daly *et al.* (2003) accounted for coastal proximity by assembling a cost grid which accounts for distance from the coast, terrain blocking, and preferred wind directions to model coastal climate modifications. Perry and Hollins (2005) used the surface area of water within a 5 km radius of each climate station as a predictive variable for gridding monthly climate surfaces for the United Kingdom. Incorporating the area of surface water around each climate station in the regression-interpolation methodology worked well in all seasons, with the exception of the summer months

In this study, we have created an interactive model for deriving gridded estimates of daily T_{min} (minimum temperature), T_{max} (maximum temperature), and precipitation for the Okanagan Basin (Figure 1). An inverse distance weighting (IDW) interpolation algorithm similar to GIDS was utilized in conjunction with regional linear and non-linear regression to generate the climate surfaces from point data. Spline interpolation was not implemented because steep temperature gradients (i.e., differences in T_{max} of 4-5 ^{o}C between stations located 500 m apart) resulted in the model creating hot and cold temperature pockets causing very large errors in the resulting temperature surfaces. This drawback of splining was also noted by Daly (2006) in a review of suitability guidelines for spatial climate datasets. In addition to latitudinal and elevation influences on temperature and precipitation, temperature inversions are accounted for using a two-layer method and lake effects are modeled by establishing the average long term temperature modification on station T_{max} values.

This study builds on past work that investigated the impacts a warmed climate could have on water resources in the Okanagan Basin (Cohen and Kulkarni, 2001; Neilsen *et al.*, 2001; Cohen *et al.*, 2006; Neilsen et al., 2006). The climate surfaces used in these studies were based on the monthly climate grids produced using PRISM. At a spatial scale of 4 and 1 km, the PRISM grids were too coarse to differentiate valley and mid-slope locations (Neilsen *et al.*, 2001; 2006).

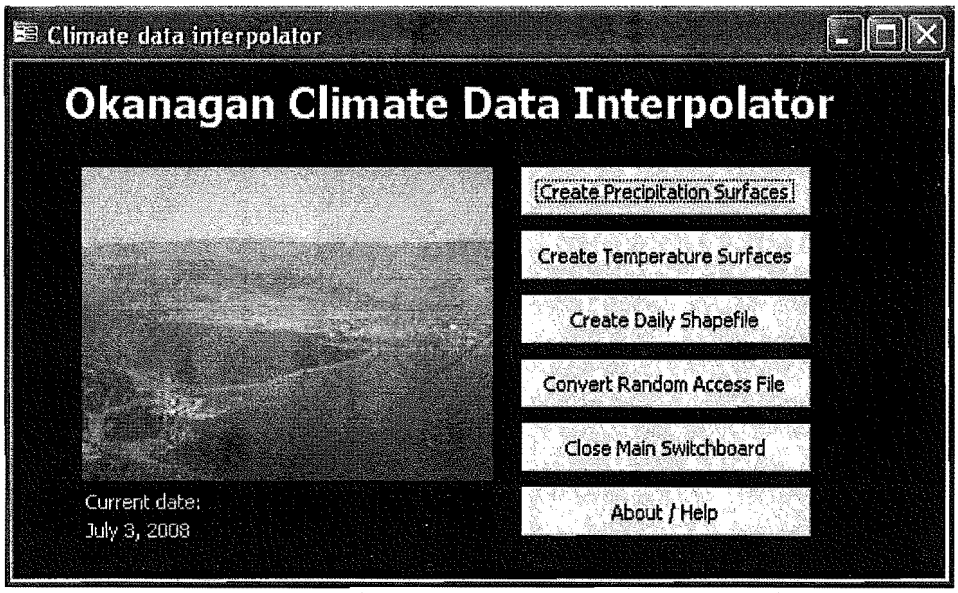

Figure 1: The Okangan Climate Data Interpolator Model splash screen.

Geographic Region

The Okanagan Basin encompasses approximately 8,000 km^2 in the southern interior of British Columbia, Canada between 48° 56' and 50° 30' North latitude and 118° 37' and 120° 22' West longitude (Figure 2). Okanagan Lake (350 m ASL) and a number of smaller 'main-stem lakes' bisect the watershed. The elevations of the surrounding mountains range from approximately 1,600 – 2,000 m asl. The region has a dry, continental climate due to its location in the rain shadow of the Coast (and Cascade) mountain ranges. On average, 88% of the 550 mm of mean annual precipitation is lost through evaporation and sublimation (Hall *et al.*, 2001). Basin averages such as those reported by Hall *et al.* (2001) mask the strong elevational and north-to-south climate gradients that extend up the 160 km valley. The southern extent of the basin is much warmer and drier than the north. There is an obvious orographic effect as average annual precipitation ranges from just under 300 mm to just over 400 mm south to north in the valley bottom, but up to 770 mm in sub-alpine regions.

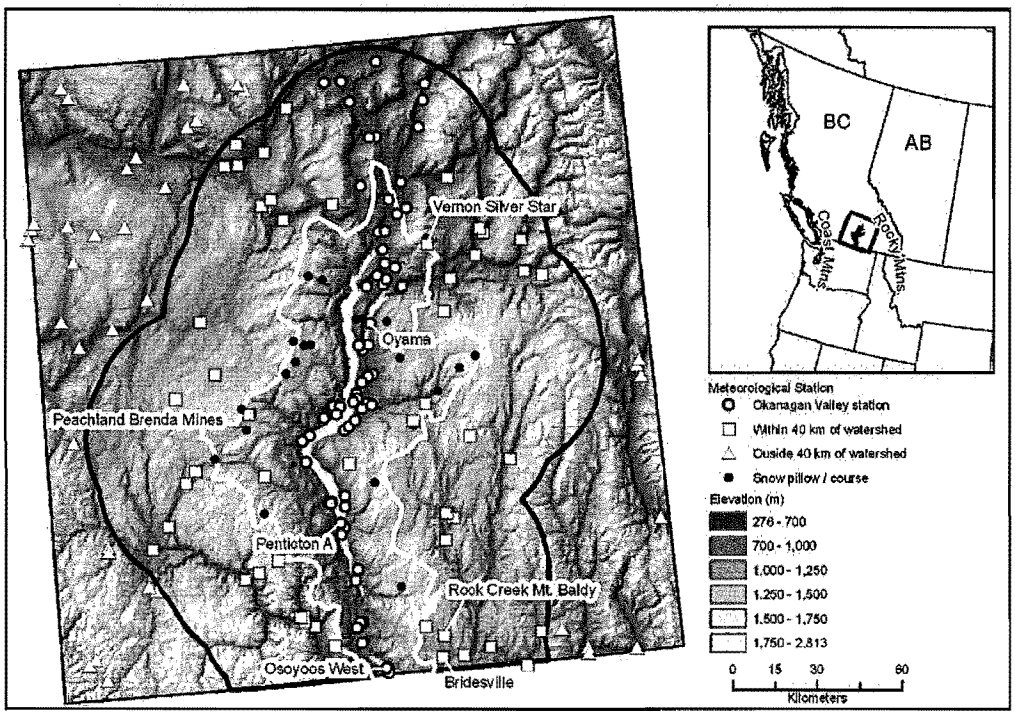

Figure 2: Okanagan valley watershed base map and study area location. Stations with labels used for cross-validation.

Climate Data

Meteorological data were acquired from the Canadian Daily Climate Data - Temperature and Precipitation CD for Western Canada (Environment Canada, 2000). In total, data from 168 stations (66 within the basin and 102 within approximately 70 km) were extracted from the data CD and used to generate a 41 year meteorological database of daily T_{max}, T_{min}, and precipitation (1960 - 2000). Since the analysis described here, data up to 2006 have been included in the model. The lack of mid-high elevation meteorological stations in the Okanagan Basin necessitated the incorporation of the stations surrounding the Okanagan valley (Figure 2) and data from other weather data networks including the BC Environment Snow Pillow stations; BC Ministry of Transportation Highways Network and the BC Ministry of Forests Fire Weather Network.

Digital Elevation Data

A digital elevation model (DEM) with a 100-m grid cell size was created as a mosaic from DMTI Spatial's (Markham, Ontario) digital database. A sensitivity analysis of grid cell size on model error indicated that the optimal spatial resolution for the climate interpolation model was 500 m. Thus, to increase computing efficiency and reduce disk storage requirements, while maintaining model integrity, the 100 m DEM was re-sampled to a grid cell size of 500 m using bilinear interpolation.

Modelling Methods

The spatial analysis involves accounting for spatial, elevation, lake effect, temperature inversion, and latitudinal variability in the meteorological data. Interpolation by inverse distance weighting (IDW) was undertaken using the Spatial Analyst feature of ArcGIS (ESRI, Redlands, CA).

Historic Temperature Grids

Daily maximum and minimum temperature grids were created using step-wise regional regression in which daily residuals of T_{max} and T_{min} are interpolated using IDW. Following the interpolation, the effect of the explanatory variables (elevation and latitude) is re-introduced to the interpolated residual grid, thereby creating a spatial representation of each variable on a daily basis. The model can be represented using Equation 1. Interpolating these climate variables after removing the effect of elevation and latitude reduces the spatial bias errors that can occur with simple regression models (e.g., Goovaerts, 2000) and incorporates a spatial interpolation component for the unexplained component of the regression models (i.e., residual data values).

$$T = (a_{(i)} \times E_{(jk)}) + (b_{(i)} \times L_{(jk)}) + y_{(i)} \quad (1)$$

Where:

$T_{(i)}$ = Daily temperature (either T_{max} or T_{min}) on day i
$a_{(i)}$ = Slope of elevation regression equation on day i
E = Elevation at grid cell jk
$b_{(i)}$ = Slope of latitude equation on day i
L = Latitude of grid cell jk
$y_{(i)}$ = Model error (residual value from interpolated grid) on day i

The elevation regression is applied if the trend is significant ($p<=0.05$) and the R^2 value is greater or equal to 0.25. The R^2 cut off was implemented to enhance the ability to detect inversions, and subsequently apply the two-layer model. Instead of extrapolating daily calculated lapse rates the constrained lapse rate approach of Stahl *et al.* (2006) was applied. Using the constrained approach default lapse rates, averaged by month, were used for grid cells in which the elevation is greater than the highest meteorological station that reported on any given day. The monthly default lapse rates were taken from Stahl *et al.* (2006) and were calculated using paired stations (Vernon Silver Star Lodge [1572 m] and Vernon Cold Stream Ranch [482 m]).

While the elevation-temperature regression are calculated using all stations within 40 km of the watershed, the latitude-temperature regression is completed using stations located along the Okanagan valley only . The remaining stations located outside of the 40 km buffer are used to reduce the likelihood that the basin boundary extends beyond all meteorological stations that reported on any given day, thereby minimizing the potential for interpolation artifacts along the watershed boundary.

Prior to the daily regression analysis the T_{max} data are adjusted to remove the average cooling/heating effect of surface water bodies for all stations within 5 km of a water body. In our study area, daily lapse rates and the occurrence of temperature inversions in the Okanagan

Valley are strongly affected by Okanagan Lake. T_{min} surfaces did not take lake effects into account because T_{min} temperatures are typically measured around 5:00 am and are a function of local topography (Bolstad *et al.*, 1998; Yoshikado and Kondo, 1989). Monthly lake induced temperature change per 10 km^2 of lake area within 5 km of the meteorological stations were derived by regressing lake area with daily observed T_{max} values using data from 1960 – 2000 (Figure 3). The approach adopted provides a simplified method to produce a conservative quantification of T_{max} modification as a result of surface water bodies.

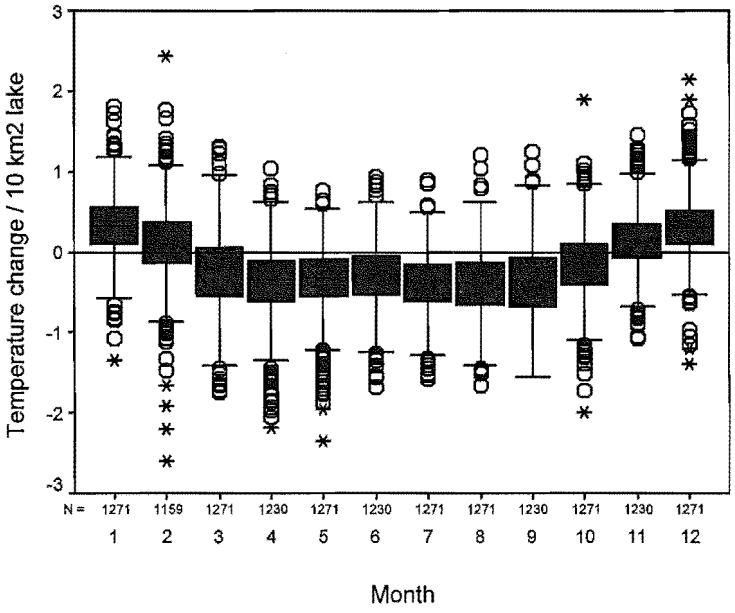

Figure 3: Predicted T_{max} difference for every 10 km^2 of adjacent lake area (January 1, 1960 – December 31, 2000). Outliers (shown with circles) are cases with values between 1.5 and 3 box lengths from the upper or lower inter-quartile range. Extremes are shown as a star.

Also of particular importance are temperature inversions that typically develop at night during clear sky conditions in mountainous terrain (Whiteman *et al.*, 2004). Using earlier versions of the model large temperature simulation errors occurred due to temperature inversions. As a result, the model incorporates a two-layer approach in which inversions (either T_{max} or T_{min}) are detected by fitting a second order polynomial to the observed data and comparing best-fit statistics with the linear regression model (Figure 4). If an inversion is detected, the observed temperature data are subset into two groups, including: 1) stations within the mixing layer (i.e., below the inversion), and 2) stations at elevations greater than the inversion height. The mixing height is defined as the elevation at which the derivative of a best-fit second order polynomial is zero. After the data are subset, the regular regression-interpolation approach is applied to the stations below the inversion. For the upper layer component a simple IDW interpolation is applied to the raw data. If fewer than 4 stations are included within the inversion the average air temperature is assigned to all locations above the inversion height.

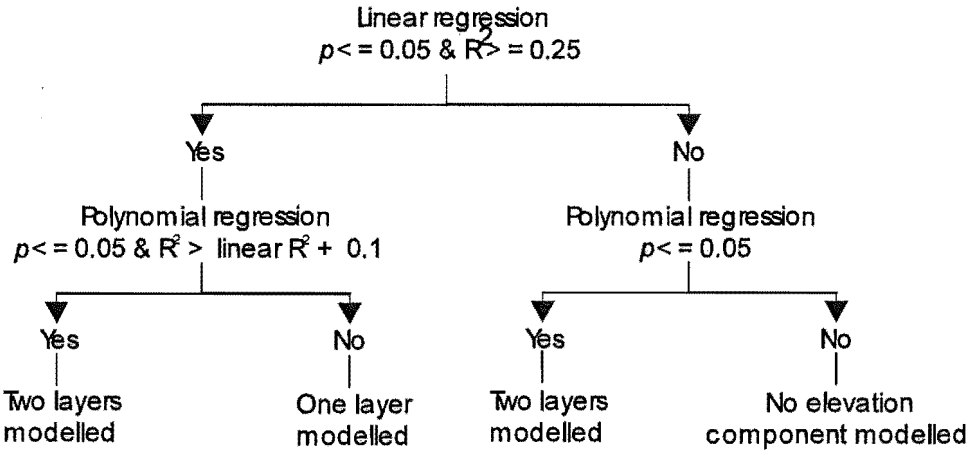

Figure 4: Model decision structure for T_{min} and T_{max} inversion and elevation-trend detection.

Historic Precipitation Grids

Gridded mean filter analysis was employed to match the scale of orographic processes in the region with the appropriate terrain representation. This analysis was completed by regressing the 41 year (1960 – 2000) average winter and early spring precipitation (December, January, February, and March) with elevation using a series of increasingly generalized DEMs. The ensemble of DEMs was generated from the average elevation within a moving grid cell window with dimensions ranging from 3-by-3 to 99-by-99 grid cells. Based on this analysis, the elevation value used should represent the average elevation surrounding each meteorological station (Spreen, 1947; Barros and Lettenmaier, 1994; Daly *et al.*, 1994; Marquinez *et al.*, 2003). Using the average elevation around each station avoids situations in which stations in narrow mountain valleys record more precipitation than their point elevations would suggest (Barry, 1981). Similarly, stations located on narrow peaks may not accumulate as much precipitation as their elevation would suggest because the blocking effect of the peak is insufficient to generate uplift and hydrometeor formation.

Daily precipitation grids were created using Equation 2. Prior to the spatial interpolation, the data were de-trended for the north-to-south precipitation gradient and the orographic component of precipitation. Again the north-to-south precipitation gradients were calculated using the Okangan Valley stations only (Figure 2). The precipitation model differs from the temperature model in that the regressions are based on monthly precipitation totals. To derive daily surfaces using monthly elevation-precipitation and latitude-precipitation relationships required the calculation of the percent of monthly precipitation at each station for each day.

$$\mathrm{Pr}_{(i)} = ([a_{(i)} \times E_{(jk)}] \times P_{(ijk)}) + ([b_{(i)} \times L_{(jk)}] \times P_{(ijk)}) + y_{(i)} \qquad (2)$$

Where:
$\mathrm{Pr}_{(i)}$ = Precipitation on day i
$a_{(i)}$ = Slope of elevation regression equation on day i
E = Elevation at grid cell jk

P = Percent of monthy precipitation observed at cell jk on day i
$b_{(i)}$ = Slope of latitude equation on day i
L = Latitude of grid cell jk
$y_{(i)}$ = Model error (residual value from interpolated grid) on day i

Two spatial interpolations are utilized, one for the residual values from the regression analysis and another to interpolate the percent of monthly precipitation on each day. Following the interpolation of daily precipitation percentages and regression model residuals using IDW, Equation 2 is reversed to create daily precipitation grids. In contrast to the one-step regression-interpolation procedures developed by Daly *et al.* (1994), Thornton (1997), Nalder and Wein (1998), and Hutchinson (1999), the spatial dependences of latitude and elevation were removed before the spatial interpolation because the daily adjustments of each observed precipitation value were based on monthly precipitation totals. The month-based approach for precipitation was favored over daily regression analysis because with so few high elevation stations, single station anomalies at a daily time-step can affect the elevation-precipitation relationship significantly. These daily anomalies could be caused by localized terrain attributes and / or atmospheric phenomenon that may not be representative over the entire study area.

Cross-validation of the interpolated climate surfaces was performed as follows. Six sites (Table 1, Figure 2) and were removed from the analysis one station at a time. The climate surfaces were derived using the remaining stations, and the interpolated data were checked against the observations for the removed stations. The mean error (ME) (predicted-observed), mean absolute error (MAE) (average of absolute values of predicted-observed), root mean square error (RMSE) (standard deviation of the ME), and linear regression statistics (simulated versus observed) were determined on a daily basis at each of the six sites for maximum daily temperature, minimum daily temperature, and precipitation for a one-year time period (July 1, 1989 – June 30, 1990). Cross-validation of the precipitation surfaces was also performed on a monthly basis because the elevation-regression models were based on monthly precipitation totals.

Table 1. Meteorological station attributes for six locations used to cross-validate the interpolated temperature and precipitation surfaces.

Station Name	Latitude	Longitude	Station Elevation (m)
Vernon Silver Star	50° 21'	119° 03'	1,572
Oyama	50° 07'	119° 22'	440
Peachland Brenda Mines	49° 52'	120° 00'	1,520
Penticton A	49° 28'	119° 36'	344
Rock Creek Mt Baldy*	49° 07'	119° 09'	1,174
Bridesville*	49° 03'	119° 10'	1,187
Osoyoos West	49° 02'	119° 27'	297

*Only precipitation validated at Rock Creek Mt. Baldy because temperature data not observed during cross-validation period. Bridesville used as the sixth station to verify temperature data in lieu of Rock Creek Mt. Baldy.

Cross-validation of the daily and monthly precipitation surfaces showed the ME, MAE, and RMSE were largest at Vernon Silver Star and Peachland Brenda Mines (Table 2; Figure 2). The large errors at these locations were attributed to the lack of neighbouring stations on the same mountain range. Rock Creek Mt. Baldy, also a mid-elevation station, did not show a similar error due to its location nearby other mid to high elevation stations (Table 2; Figure 2). The

dependency of empirical regression analysis on the few high elevation stations is well documented and a common problem in alpine environments (Running *et al.*, 1987; Daly *et al.*, 1994; Lookingbill and Urban, 2003). For the daily data the ME was closer to zero than the MAE for all stations, indicating that the errors were distributed around zero. With slopes near 1, y-intercepts near 0, and high R^2 values the monthly regression statistics for 5 out of 6 stations indicate that the precipitation error was small over the course of each month.

Table 2: Comparison of Mean Error (predicted minus observed), Mean Absolute Error (average of errors after the errors are made positive), Root Mean Square Error (standard deviation of the errors), and linear regression statistics based on daily and monthly precipitation totals for six locations.

Comparison Method	Vernon Silver Star	Oyama	Peachland Brenda Mines	Penticton A	Rock Creek Mt. Baldy	Osoyoos West
Daily						
ME (mm)	-0.9	0.1	0.2	0.0	0.2	0.2
MAE (mm)	1.7	0.5	1.6	0.9	0.9	0.5
RMSE (mm)	3.7	1.1	3.2	2.3	2.2	1.9
Slope	0.58	0.88	0.87	0.63	0.78	1.07
Y-intercept	0.37	0.19	0.46	0.41	0.54	0.18
R^2	0.58	0.84	0.53	0.60	0.68	0.69
Monthly						
ME (mm)	-25.3	2.0	6.0	-0.8	5.0	7.5
MAE (mm)	25.9	3.9	12.1	5.4	9.1	7.8
RMSE (mm)	23.6	4.7	13.8	8.2	9.9	9.4
Slope	0.66	1.03	1.17	0.90	0.95	1.13
Y-intercept	4.24	1.19	-4.57	2.97	7.36	-2.40
R^2	0.88	0.97	0.89	0.91	0.93	0.98

Cross-validation of the predicted temperature surfaces indicates that, on average, the daily maximum temperature surfaces were more accurate than the minimum temperature surfaces (Table 3). The higher T_{min} error was likely because there were more days when no distinguishable minimum temperature lapse rate was found (Figure 5). The weak relationship between minimum daily temperatures and elevation is likely due to the drainage of cold air from mid and high elevations into valley bottoms, which leads to the formation of atmospheric inversions (Cox, 1920; Barry, 1981; Whiteman *et al.*, 2004). The negative ME, low regression slope, and negative y-intercept for T_{min} at the high elevation stations Vernon Silver Star and Peachland Brenda Mines indicates that the predicted minimum temperatures were lower than observed, which would contribute to conservative snow pack melt rates. The relatively small ME for the low elevation stations (i.e., Oyama, Penticton A, Osoyoos West) is an indication that the 500 m grid cell size used in this study is an advantage over the 4 and 1 km temperature grids that were used for the crop water demand study conducted by Neilsen *et al.* (2001;2006).

Table 3: Comparison of Mean Error (predicted minus observed), Mean Absolute Error (average of errors after the errors are made positive), Root Mean Square Error (standard deviation of the errors), and linear regression statistics based on daily maximum and minimum temperatures for six locations.

Comparison Method	Vernon Silver Star	Oyama	Peachland Brenda Mines	Penticton A	Bridesville	Osoyoos West
Max. Daily Temp.						
ME (°C)	1.0	-0.1	0.8	-0.2	1.5	0.9
MAE (°C)	1.7	0.7	1.5	0.7	1.8	1.0
RMSE (°C)	2.0	1.0	1.8	0.9	1.5	0.8
Slope	0.99	1.01	0.98	1.03	0.99	1.04
Y-intercept	1.09	-0.18	0.96	-0.56	1.69	0.25
R^2	0.96	0.99	0.96	0.99	0.98	0.99
Min. Daily Temp.						
ME (°C)	-2.0	-1.1	-1.8	0.4	1.0	-0.1
MAE (°C)	2.5	1.2	2.4	1.2	1.7	0.6
RMSE (°C)	2.5	1.0	2.3	1.4	1.9	0.9
Slope	0.87	0.96	0.87	0.95	0.90	0.97
Y-intercept	-2.20	-0.90	-1.9	0.59	0.91	0.08
R^2	0.90	0.97	0.89	0.96	0.93	0.98

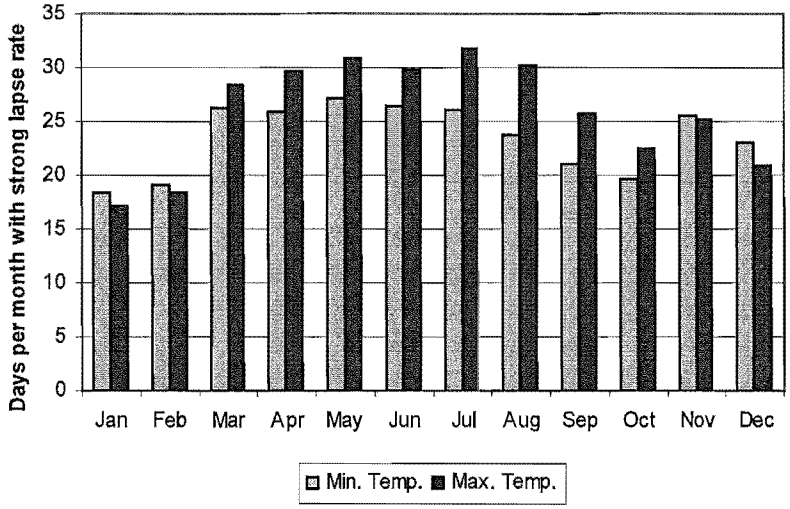

Figure 5: Average monthly frequency of strong lapse rates (p<=0.05 and $R^2 \geq 0.25$) observed using linear regression analysis of daily temperatures and climate station elevation from August 1, 1960 – July 31, 1990.

Future Climate Surfaces

Future daily temperature and precipitation surfaces were developed using multiple Global Climate Models (GCMs) and 3 IPCC greenhouse gas emissions scenarios (SRES). The six GCMs used were CGCM2, CGCM3, CM2.1, ECHAM5, HadCM3, PCM1. The SRES scenarios included A2 which describes a very heterogeneous world with high population growth, slow economic development and slow technological change; B1 which describes a convergent world, with a global population that peaks in mid-century with rapid changes in economic structures

toward a service and information economy and B2 which describes a world with intermediate population and economic growth, emphasising local solutions to economic, social, and environmental sustainability. No likelihood has been attached to any of the SRES scenarios (IPCC, 2008).

Data were downscaled to 500 x 500m grid cells using TreeGen (Cannon, 2008) a model which combines a synoptic variable classification scheme (Cannon et al., 2002) with a weather generator. In this way, observed synoptic-scale atmospheric predictor variables are related to observed surface weather variables, and then, based on these relationships, realistic series of weather variables are generated from GCM synoptic scale variables. Algorithm details are given in Stahl *et al.* (2008, Appendix A). Predictors in the classification model were mean sea-level pressure surface air temperature, and surface precipitation data from the US NCEP/NCAR model reanalysis (Kalnay *et al.*, 1996). Daily mean maps from 1948-2006 were obtained for a region covering western North America and the North Pacific Ocean (30°N-70°N; 160°W-110°W). Data were sub-sampled from the 2.5° by 2.5° resolution grid to a 5° by 7.5° grid to facilitate later use with coarser spatial resolution GCM data. Synoptic-scale fields matching those from the NCEP/NCAR Reanalysis were obtained from transient greenhouse gas plus aerosol runs of were CGCM2, CGCM3, CM2.1, ECHAM5, HadCM3, PCM1 for simulated years 1961–2100 with forcing variables from the A2 SRES scenario and one of the B1 or B2 SRES scenarios. Concurrent daily weather conditions in the Okanagan Valley were represented by precipitation amounts, mean temperatures, and diurnal temperature ranges at major surface stations. The "stations" in this case are a subset of points from the gridded climate field. Derived climate normal variables at all points in the basin were first clustered and were used to split the area into a series of homogeneous climate regions. Finally, the grid points nearest to the cluster centroids served as stations in the downscaling.

The Okanagan Climate Data Model (Figure 1) has been used to drive the Okanagan Irrigation Water Demand Model, which provides calculations of Penman Monteith reference ET and a range of agro-climatic indices for each climate grid cell in addition to crop and terrain based irrigation water demand.

References

Barros, A.P., and D.P. Lettenmaier (1994), Dynamic modeling of orographically induced precipitation, *Rev. Geophys., 32* (3), 265-284.

Barry, R.G. (1981), *Mountain weather and climate,* Methuen, London. 313 pp.

Bolstad, P.V., L. Swift, F. Collins, and J. Regniere (1998), Measured and predicted air temperature at basin to regional scales in the southern Appalachian mountains, *Agr. Forest Meteorol., 91*, 161-176.

Cannon, A.J., and Whitfield, P.H. (2002), Synoptic map classification using recursive partitioning and principle component analysis. *Monthly Weather Rev.* 130:1187-1206.

Cannon, A.J. (2008), Probabilistic multi-site precipitation downscaling by an expanded Bernoulli-gamma density network. *Journal of Hydrometeorology.* http://dx.doi.org/10.1175%2F2008JHM960.1

Cohen, S., and T. Kulkarni (2001), *Water management & climate change in the Okanagan Basin. Environment Canada & University of British Columbia.* Project A206, submitted to the

Adaptation Liaison Office, Climate Change Action Fund, Natural Resources Canada, Ottawa, 75 pp.

Cohen S., D. Neilsen, and R. Welbourn (2004), Expanding the dialogue on climate change & water management in the Okangan Basin, British Columbia, Project A463/433, submitted to the Adaptation Liaison Office, Climate Change Action Fund, Natural Resources Canada, Ottawa, 257 pp.

Cohen, S., D.Neilsen, S. Smith, T. Neale, B. Taylor, M. Barton, W. Merritt, Y. Alila, P. Shepherd, R. McNeill, J. Tansey, J. Carmichael and S. Langsdale (2006), Learning with local help: Expanding the dialogue on climate change and water management in the Okanagan Region, British Columbia, Canada. *Climatic Change 75*:331-358.

Cox, H.J. (1920), Weather conditions and thermal belts in the North Carolina mountain region and their relation to fruit growing, *Ann. Assoc. Am.Geogr., 10*, 57-68.

Daly, C., R.P. Neilson, and D.L. Phillips (1994), A statistical-topographic model for mapping climatological precipitation over mountainous terrain, *J. Appl. Meteorol., 33*, 140-158.

Daly, C., E. H. Helmer, and M. Quinones (2003), Mapping the climate of Puerto Rico, Vieques and Culebra, *Int. J. Clim., 23*, 1359-1381.

Daly, C. (2006), Guidelines for assessing the suitability of spatial climate data sets, *Int. J. Clim., 26*, 707-721.

Environment Canada (2002), *Canadian daily climate data*, CDCD V1.01, Climate Information Branch, Atmospheric Environmental Service. Ottawa, Ontario, Canada.

Goovaerts, P. (2000), Geostatistical approaches for incorporating elevation into spatial interpolation of rainfall, *J. Hydrol., 228*, 113-129.

Hall, K., J. Stockner, N. Schreier, and R. Bestbier (2001), *Nutrient sources and ecological impacts on Okanagan Lake*. Institute for Resources and Environment, University of British Columbia, Vancouver, British Columbia.

Hutchinson, M.F. (1995), Interpolating mean rainfall using thin plate smoothing splines, *Int. J. GIS, 9*, 385-403.

Hutchinson, M.F. (1999), ANUSPLIN Version 4.0, Australian National University, Canberra, Australia, http://cres.anu.edu.au/software/anusplin.html.

Intergovernmental Panel on Climate Change (IPCC) (2008), Fourth Assessment Report –AR4. http://www.ipcc.ch/ipccreports/ar4-syr.htm

Kalnay, E., M. Kanamitsu, R. Kistler, W. Collins, D. Deaven, L. Gandin, M. Iredell, S. Saha, G. White, J. Woolen, Y. Zhu, M. Chelliah, W. Ebisuzaki, W. Higgins, J. Janowiak, K. C. Mo, C. Ropelewski, J. Wang, A. Leetma, R. Reynolds, R. Jenne, and D. Joseph, (1996), The NCEP/NCAR 40-year reanalysis project. *Bulletin of the American Meteorological Society*, 77, 437-471.

Lookingbill, T.R., and D.L. Urban (2003), Spatial estimation of air temperature differences for landscape-scale studies in montane environments, *Agr. Forest Meteorol., 114*, 141-151.

Marquinez, J., J. Lastra, and P. Garcia (2003), Estimation models for precipitation in mountainous regions: the use of GIS and multivariate analysis, *J. Hydrol., 270*, 1-11.

Nalder, I.A., and R.W. Wein (1998), Spatial interpolation of climate Normals: test of a new method in the Canadian boreal forest, *Agr. Forest Meteorol., 92*, 211-225.

Neilsen, D., S. Smith, W. Koch., G. Frank, and J. Hall (2001), Impact of climate change on crop water demand and crop suitability in the Okanagan Valley, British Columbia. *Technical Bulletin 01-15,* 32 pp., Pacific Agri-Food Research Centre, Summerland, BC, Canada.

Neilsen, D., S. Smith, G., Frank, W. Koch, Y. Alila, W. Merritt, B. Taylor, M. Barton, J. Hall, and S. Cohen (2006), Potential impacts of climate change on water availability for crops in the Okanagan Basin, British Columbia. *Can. J. Soil Sci. 86*: 909-924

Perry, M., and D. Hollins, (2005), The generation of monthly gridded datasets for a range of climatic variables over the UK, *Int. J. Climatol.*, 25, 1041-1054.

Running, S., R. Nemani, and R. Hungerford (1987), Extrapolation of synoptic meteorological data in mountainous terrain and its use for simulating forest evapotranspiration and photosynthesis, *Can. J. Forest Res., 17*, 472-483.

Simpson, J. J., G. L. Hufford, C. Daly, J. S. Berg, and M. D. Fleming (2005), Comparing maps of mean monthly surface temperature and precipitation for Alaska and adjacent areas of Canada produced by two different methods, *Arctic, 58* (2), 137-161.

Spreen, W.C. (1947), A determination of the effect of topography upon precipitation, *EOS T. Am. Geophys. Un., 28*(2), 285-290.

Stahl, K., R. D. Moore, J. A. Floyer, M. G. Asplin, and I. G. McKendry (2006), Comparison of approaches for spatial interpolation of dialy air temperature in a large region with complex topography and highly variable station density, *Ag. Forest Meteorol., 139*, 224-236.

Stahl, K., R. D. Moore, J. M. Shea, D. Hutchinson, and A. J. Cannon (2008), Coupled modelling of glacier and streamflow response to future climate scenarios. Water Resour. Res., 44, W02422, doi:10.1029/2007WR005956.

Thornton, P.E., S.W. Running, M.A. White (1997), Generating surfaces of daily meteorological variables over large regions of complex terrain, *J. Hydrol., 190*, 214-251.

Whiteman, C.D., B. Pospichal, S. Eisenbach, P. Weihs, C.B. Clements, R. Steinacker, E. Mursch-Radlgruber, and M. Dorninger (2004), Inversion breakup in small Rocky Mountain and alpine basins, *J. Meteorol., 43*, 1069-1082.

Yoshikado, H., and H. Kondo (1989), Inland penetration of the sea breeze over the suburban area of Tokyo, *Boundary-Layer. Meteorol., 48*, 389-407.